STRUCTURE ANISOTROPY IN MHD TURBULENCE SUBJECTED TO MEAN SHEAR AND FRAME ROTATION

Stavros C. Kassinos
Dept. of Mechanical and Manufacturing Engineering,
University of Cyprus
Nicosia, Cyprus
and Department of Mechanical Engineering, Stanford University
Stanford, CA 94305
kassinos@ucy.ac.cy

Alan Wray
Center for Turbulence Research
NASA Ames Research Center
aawray@mail.arc.nasa.gov

ABSTRACT

We consider homogeneous turbulence in a conducting fluid that is exposed to a uniform external magnetic field while being sheared in fixed and rotating frames. We take both the frame-rotation axis and the applied magnetic field to be aligned in the direction normal to the plane of the mean shear. We find that a key parameter determining the structural morphology of the flow is the ratio of the time scale of the mean shear to the Joule time, $\tau_{\text{shear}}/\tau_m$. When $\tau_{\text{shear}} << \tau_m$, we find that the turbulence structures tend to align preferentially with the streamwise direction irrespective of the magnetic Reynolds number, R_m. When $\tau_{\text{shear}} >> \tau_m$, we find that at low R_m the turbulent eddies become elongated and aligned with the magnetic field, but at moderately high R_m, there is partial streamwise alignment of the eddies. When $\tau_{\text{shear}} \approx \tau_m$, we find that competing mechanisms tend to produce different structural anisotropies, and small variations in dimensionless parameters can have a strong effect on the structure of the evolving flow. For example, at $R_m << 1$, a preferential alignment of structures in the direction of the magnetic field emerges as the flow evolves, consistent with the predictions of the quasi-static approach. For $R_m \sim 1$, the structures are found to be equally aligned in the streamwise and spanwise direction at large times. However, when R_m is moderately high ($10 \lesssim R_m \lesssim 50$) this strong spanwise alignment is replaced by a preferential alignment of structures in the streamwise direction. Counter to intuition, we found evidence that strong rotation in combination with a spanwise magnetic field tends to promote a streamwise alignment of the eddies, at least when $\tau_{\text{shear}} \approx \tau_m$.

1. INTRODUCTION

The combined effects of system rotation and mean shear on magnetohydrodynamic turbulence exposed to an external magnetic field are important in a number of physical phenomena and engineering applications. Examples include phenomena such as the accretion of Keplerian disks and the Earth's dynamo, and applications such as plasma flows associated with fusion, magnetic steering technologies, and magnetogasdynamic (MGD) schemes for flow control and propulsion in advanced hypersonic vehicles. For Keplerian disks to accrete a source of enhanced angular momentum transport must be present in the disk. A key issue is whether, in the absence of stirring, hydrodynamic shear turbulence can be self-sustaining in Keplerian disks, or whether some additional mechanism, such as magnetic fields and thermal stratification must also be active. From an engineering point of view, many of the CFD codes used for the prediction of MHD and MGD flows rely on simple turbulence closures, like k-ϵ models, with additional ad hoc modifications to account for the effects of the magnetic field. Such closures neglect the important dynamical role that the structure of the turbulence plays in the interaction between the flow and the applied magnetic field, and as a result they lack generality and robustness.

At a fundamental level it is well known that, when acting alone, mean shear, frame rotation, and external magnetic fields modify the turbulence structure and induce strong anisotropy. Mean shear tends to produce long streamwise eddies, frame rotation tends to produce long columnar structures aligned with the rotation axis, and magnetic fields, through the action of the Lorentz force, produce structure elongation along the direction of the field. Despite the importance of MHD turbulent shear flows in both our physical environment and in our technology, our understanding of the structure modifications that take place when all three effects act concurrently is at best incomplete. This can be attributed partly to the lack of modern, high resolution simulations of these flows.

In this work, we have been carrying out a series of large-scale direct numerical simulations that aim to answer some of the questions raised above. Our goal is to understand the mechanisms that lead to instability and structural anisotropy when the combined effects of mean shear, system rotation and external magnetic fields act concurrently on homogeneous turbulence. We hope that this understanding will enable us to develop improved turbulence closures for MHD applications.

1.1 The Structure in the Case of Hydrodynamic Shear

In the purely hydrodynamic case, it is well documented that

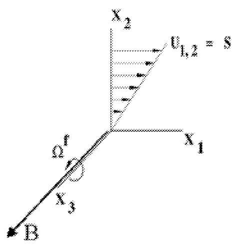

Figure 1: Configuration for shear in a rotating frame. Here B denotes the external magnetic field (when applicable), Ω^f the frame rotation rate, and S the shear rate.

mean shear tends to elongate and align the turbulence structures in the direction of the mean flow (Rogers and Moin, 1987) and that frame rotation can act to either stabilize or destabilize homogeneous shear flow. For homogeneous turbulence that is being sheared in a rotating frame (see Fig.1), the morphology of the structure depends weakly on the ratio of the frame rotation rate to the mean shear rate, but in general a preferential streamwise alignment of the turbulent eddies is maintained.

1.2 The Structure of Undeformed MHD turbulence

For vanishingly small magnetic Reynolds numbers ($R_m \ll 1$), and in the absence of mean shear or frame rotation, the induced magnetic fluctuations are much weaker than the applied field and their characteristic time scale, based on their diffusion, is much shorter than the eddy turnover time. A classical approximation for undeformed MHD turbulence at low R_m is the Quasi-Static (QS) approximation. In this approximation, the induced magnetic field fluctuations become a linear function of the velocity field. Kassinos et al. (2002) and Knaepen et al. (2004) considered the case of initially isotropic decaying MHD turbulence, and concluded that the QS approximation was reasonably accurate for $R_m \lesssim 1$. For higher R_m, where the QS approximation fails, they proposed the use of the Quasi-Linear (QL) approximation, which amounts to retaining the unsteady term in the magnetic induction equation, retaining the non-linear hydrodynamic terms in the fluctuating momentum equation, but dropping all the nonlinear terms involving the magnetic fluctuations. They carried out a series of DNS and concluded that in unstrained MHD turbulence the QL approximation was valid for the entire range of magnetic Reynolds numbers they examined ($R_m \lesssim 30$).

1.3 The Structure of Sheared and rotating MHD turbulence

Surprisingly, little work has been done to explore the structure of homogeneous MHD turbulence under the influence of mean shear and frame rotation. The objective of this work is to use DNS to probe the fundamental physics in sheared MHD turbulence. Primarily, we are interested in understanding the effects of shear and rotation on the dynamics of MHD turbulence, including the structural morphology and stability of these flows. Stability modifications due to the presence of the magnetic field can potentially have implications for the evolution of stellar accretion disks and they constitute an important effect that must be built into a successful model for MHD turbulence.

We start by discussing the relevant dimensionless parameters that characterize MHD and MGD flows in the presence of mean shear and frame rotation. In Section 3 we introduce the governing equations for ideal MHD. The numerical code and associated initial conditions are described in Section 4, while Section 5 is devoted to a discussion of the most important results. A concluding summary is given in Section 6.

2. DIMENSIONLESS PARAMETERS

The effects of a uniform magnetic field applied to unstrained homogeneous turbulence in an electrically conductive fluid are characterized by three dimensionless parameters. The first of these is the magnetic Reynolds number

$$R_m = \frac{vL}{\eta} = (\frac{v}{L})(\frac{L^2}{\eta}), \tag{1}$$

where L is the integral length scale and v is the r.m.s. fluctuating velocity

$$v = \sqrt{R_{ii}/3}, \qquad R_{ij} = \overline{u_i u_j}. \tag{2}$$

Here u_i is the fluctuating velocity, and η is the magnetic diffusivity

$$\eta = 1/(\sigma\mu^*) \tag{3}$$

where σ is the electric conductivity of the fluid, and μ^* is the fluid magnetic permeability (here we use μ^* for the magnetic permeability and reserve μ for the dynamic viscosity). Thus the magnetic Reynolds number represents the ratio of the characteristic time scale for diffusion of the magnetic field to the time scale of the turbulence. In the case of vanishingly small R_m, the distortion of the magnetic field lines by the fluid turbulence is sufficiently small that the induced magnetic fluctuations $\mathbf{b}$ around the mean (imposed) magnetic field $\mathbf{B}$ are also small.

The second parameter is the magnetic Prandtl number representing the ratio of R_m to the hydrodynamic Reynolds number Re_L

$$P_m \equiv \frac{\nu}{\eta} = \frac{R_m}{Re_L}, \qquad Re_L = \frac{vL}{\nu}. \tag{4}$$

The magnetic-interaction number (or Stuart number) is

$$N \equiv \frac{\sigma B^2 L}{\rho v} = \frac{(B^{\text{ext}})^2}{\eta}\frac{L}{v} = \frac{\tau}{\tau_m}, \tag{5}$$

where B is the magnitude of the magnetic field, $B^{\text{ext}} = B/\sqrt{\mu^*\rho}$ is the magnetic field expressed in Alfven units, and ρ is the fluid density. N represents the ratio of the large-eddy turnover time τ to the Joule time τ_m, i.e. the characteristic time scale for dissipation of turbulent kinetic energy by the action of the Lorentz force. N parametrizes the ability of an imposed magnetic field to drive the turbulence to a two-dimensional three-component state. In the absence of mean shear and frame rotation, the continuous action of the Lorentz force tends to concentrate energy in modes independent of the coordinate direction aligned with $\mathbf{B}$. As a two-dimensional state is approached, Joule dissipation decreases because fewer and fewer modes with gradients in the direction of $\mathbf{B}$ are left available. In addition, the tendency towards two-dimensionality and anisotropy is continuously opposed by non-linear angular energy transfer from modes perpendicular to $\mathbf{B}$ to other modes, which tends to restore isotropy. If N is larger than some critical value N_c, the Lorentz force is able to drive the turbulence to a state of complete two-dimensionality.

For smaller N, the Joule dissipation is balanced by non-linear transfer before a complete two-dimensionality is reached. For very small N ($N \leq 1$), the anisotropy induced by the Joule dissipation is negligible. Here we take the initial value of magnetic interaction number to be $N_0 = 0$.

In the presence of mean shear and frame rotation, two additional parameters become important. The first of these is the ratio of the time scale of the mean shear to the Joule time τ_m,

$$M \equiv \frac{(B^{\rm ext})^2}{\eta S} = \frac{\tau_{\rm shear}}{\tau_m} \tag{6}$$

where S is the mean shear rate. The second is the ratio of the frame rotation rate Ω^f to shear rate S,

$$\lambda \equiv \frac{\Omega^f}{S} \tag{7}$$

where $\Omega^f = -\Omega^f_{12}$ so that positive values of λ correspond to a frame counter-rotating relative to the sense of rotation associated with the mean shear (see Fig. 1).

3. GOVERNING EQUATIONS

Transport in homogeneous MHD shear flow is described by the incompressible MHD equations

$$\tilde{u}_{i,i} = 0 \qquad \tilde{b}_{i,i} = 0 \tag{8}$$

$$\partial_t \tilde{u}_i + \tilde{u}_s \tilde{u}_{i,s} = -\frac{1}{\rho} P^*_{,i} + \tilde{b}_{i,m}\tilde{b}_m + \nu \tilde{u}_{i,ss} \tag{9}$$

$$\partial_t \tilde{b}_i + \tilde{u}_s \tilde{b}_{i,s} = \tilde{b}_s \tilde{u}_{i,s} + \eta \tilde{b}_{i,ss} \tag{10}$$

where P^* is the total pressure including magnetic contributions, $\tilde{b}_i$ is the magnetic field in Alfven units, and $\tilde{u}_i$ are the velocity components. Next, the flow variables are transformed into a rotating frame, where they are explicitly decomposed into a mean and a fluctuating part. We solve the resulting governing equations for the fluctuation fields in a coordinate system that deforms with the mean flow so that Fourier decomposition methods can be employed. In this deforming coordinate system, the transformed equations become

$$\begin{aligned} \partial_t v_i + G_{ik} v_k + \frac{\partial v_i}{\partial x_m} v_k A_{mk} + 2\Omega^f_{ik} v_k = -\frac{1}{\rho}\frac{\partial p}{\partial x_m} A_{mi} \\ + \frac{\partial B^{\rm ext}_i}{\partial x_m} b_k A_{mk} + \frac{\partial b_i}{\partial x_m} B^{\rm ext}_k A_{mk} + \frac{\partial b_i}{\partial x_m} b_k A_{mk} \\ + \nu \frac{\partial^2 v_i}{\partial x_k \partial x_z} A_{zp} A_{kp} \end{aligned} \tag{11}$$

and

$$\begin{aligned} \partial_t b_i - G_{ik} b_k = -v_k \frac{\partial B^{\rm ext}_i}{\partial x_m} A_{mk} - v_k \frac{\partial b_i}{\partial x_m} A_{mk} \\ + B^{\rm ext}_k \frac{\partial v_i}{\partial x_m} A_{mk} + b_k \frac{\partial v_i}{\partial x_m} A_{mk} + \eta \frac{\partial^2 b_i}{\partial x_k \partial x_z} A_{zp} A_{kp} \,. \end{aligned} \tag{12}$$

Here, v_i and b_i are the components of velocity and magnetic fluctuation fields transformed in the rotating frame, x_i are deforming coordinates, $G_{ij} = U_{i,j}$ is the mean velocity gradient tensor, and A_{ij} is the (Rogallo) transformation matrix satisfying

$$\dot{A}_{iz} + A_{ij} G_{jz} = 0 \,. \tag{13}$$

Table 1: Turbulence characteristics of the initial velocity field. All quantities are in MKS units.

Resolution	256^3
Box size ($\ell_x \times \ell_y \times \ell_z$)	$2\pi \times 2\pi \times 2\pi$
Rms velocity (v)	3.099
Viscosity	0.006
Integral length-scale	
$3\pi/4 \times (\int k^{-1} E(k)dk / \int E(k)dk)$	0.322
$Re = uL/v$	166
Dissipation (ϵ)	47.876
Dissipation scale ($\gamma = (\nu^3/\epsilon)^{(1/4)}$)	0.0082
$k_{\max}\gamma$	1.82
Microscale Reynolds number	
($Re_\lambda = \sqrt{15/(\nu\epsilon)} u^2$)	69.40
Eddy turnover time ($\tau = (3/2)u/\epsilon$)	0.097

In the hydrodynamic case, one can impose any mean strain tensor, but once the mean strain is specified, the homogeneity requirement imposes constraints on the evolution of the mean rotation tensor. In the MHD case, these constraints involve gradients of the mean magnetic field as well. However, when the frame rotation axis and the uniform mean magnetic field vector are perpendicular to the plane of shear, these constraints leave the mean rotation unmodified and need not be considered.

4. NUMERICAL CODE AND INITIAL CONDITIONS

We have used a pseudo-spectral code with the ability to simulate the full MHD equations (11) and (12). The numerical method used to solve the governing equations for homogeneous shear flows is similar to that introduced by Rogallo (1981). The governing equations are transformed to a set of coordinates which deform with the mean flow. This allows Fourier pseudo-spectral methods, with periodic boundary conditions, to be used for the representation of the spatial variation of the flow variables. Time advance is accomplished by a third-order Runge-Kutta method. Since the mean imposed shear skews the computational grid with time, periodic remeshing of the grid is needed in order to allow the simulation to progress to large total shear, where a self-preserving regime might be expected to prevail. The periodic remeshing introduces aliasing errors that are removed by a de-aliasing procedure included in the code. An MPI based version of the code has been implemented in the Vectoral language and tested individually for accuracy, grid independence, and scalability.

All the runs presented here have a resolution of 256^3 Fourier modes in a $(2\pi)^3$ computational domain. The initial conditions for the velocity were common to all cases. They were created starting with a pulse of energy at low wave numbers in Fourier space and a random distribution of phases for the Fourier modes. In order to let the higher-order statistics develop, the flow was evolved in the absence of mean shear or frame rotation and without a mean magnetic field, while forcing was being applied to the low wave number region of the spectrum. This initial phase was continued until an equilibrium state was reached and the skewness acquired its peak value. At that time, hereafter referred to as t_0, the external magnetic field, mean shear and frame rotation were switched on while the artificial forcing was eliminated. The characteristics of the initial field at time t_0 are summarized in Table 1.

Table 2: Parameter values for the runs considered here.

Case	η	B^{ext}	N_0	R_{m0}	M	λ
C1.2.1	1.000	9.800	10	1	0.1	$0,\frac{1}{4}$
C1.2.30	0.033	1.789	10	30	0.1	$0,\frac{1}{4}$
C2.2.1	1.000	9.800	10	1	2	$0,\frac{1}{4},\frac{1}{2},\frac{3}{4},1$
C2.2.30	0.033	1.789	10	30	2	$0,\frac{1}{4},\frac{1}{2},\frac{3}{4},1$
C2.2.50	0.020	1.386	10	50	2	$0,\frac{1}{4},\frac{1}{2},\frac{3}{4},1$
C3.2.1	1.000	9.800	10	1	20	$0,\frac{1}{4}$
C3.2.30	0.033	1.789	10	30	20	$0,\frac{1}{4}$

In the MHD runs, an initial condition for b_i has to be chosen at $t = t_0$. Here we have made the choice $b_i(t_0) = 0$. In other words, our simulations describe the response of an initially non-magnetized turbulent conductive fluid to the application of a mean magnetic field. The corresponding completely-linearized problem in the absence of mean shear and frame rotation has been described in detail in Moffatt (1967).

4.1 Parameters

In order to distinguish between our numerical runs, we will vary the initial magnetic Reynolds number R_{m0}, the initial magnetic interaction number N_0, the ratio of the timescale of the mean shear to that for magnetic diffusion M, and the ratio of the frame rotation rate to the mean shear rate λ. Specification of R_m and N completely determines η and B^{ext} according to:

$$B^{\text{ext}} = \frac{Nv^2}{R_m}, \qquad \eta = \frac{vL}{R_m}\,. \tag{14}$$

The values of these parameters for the different runs considered are summarized in Table 2.

The name convention for the cases listed in Table 2 is based on the value of M, the Magnetic Stuart number N_0, and the magnetic Reynolds number R_{m0}. Thus, the identification number of run CX.Y.Z can be interpreted as follows:

$$\begin{aligned} X = 1 \Rightarrow M_0 = 0.1 \quad X = 2 \Rightarrow M_0 = 2 \quad X = 3 \Rightarrow M_0 = 20 \\ Y = 1 \Rightarrow N_0 = 1 \quad Y = 2 \Rightarrow N_0 = 10 \end{aligned} \tag{15}$$

and where Z is such that $R_m = Z$. Thus, for the first two runs we have $M = 0.1$; for the next three $M = 2$, and finally, for the last two runs we have $M = 20$. In all cases $N_0 = 0$.

5. RESULTS

In this section we discuss some of the more important results obtained by carrying out the simulations described in the previous sections.

5.1 Eddy alignment

The effects of mean shear, frame rotation, and external magnetic fields on the turbulence structure are well understood whenever these act independently. Mean shear tends to stretch and align the turbulent eddies in the streamwise direction, strong rotation tends to induce columnar structures aligned with the rotation axis, while the action of the Lorentz force tends, through Joule dissipation, to promote long structures aligned with the mean magnetic field. Here, we examine

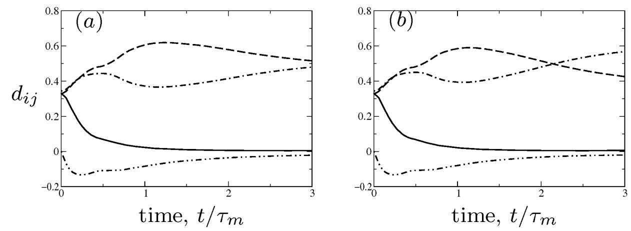

Figure 2: Structure anisotropy as measured by d_{ij} (see 16) in homogeneous MHD turbulence being sheared in a fixed frame ($\lambda = 0$) for the case with $M = \tau_{\text{shear}}/\tau_m = 0.1$: ——— d_{11}; – – – – d_{22}; —·— d_{33}; —··— d_{12}. (a) Case C121 with $R_m = 1, N = 10$; (b) Case C1230 with $R_m = 30, N = 10$. The induced structural anisotropy is completely determined by the mean shear and is independent of the magnetic Reynolds.

eddy alignment under the combined action of S, Ω^f and B^{ext}. We will first look at a series of simulations in a fixed frame (zero frame rotation) in an effort to establish the effects of the simultaneous action of the mean shear and a mean spanwise magnetic field on the turbulence structure. Then we will look at these effects in a frame rotating about a spanwise axis.

The diagnostic tool used to determine eddy alignment is the structure dimensionality tensor (Kassinos et al., 2001), which for homogeneous turbulence is defined by

$$D_{ij} = \int E(k)\,\frac{k_i k_j}{k^2}\,d^3\mathbf{k} \quad d_{ij} = D_{ij}/D_{kk} \quad D_{kk} = q^2 = 2k\,. \tag{16}$$

Note that each diagonal component of d_{ij} can attain values only between 0 and 1, and that for turbulence in which the energy-containing structures are elongated in the x_α direction, $d_{\alpha\alpha} \to 0$. On the other hand $d_{\alpha\alpha} \to 1$ corresponds to structures that are narrow and have strong gradients in the x_α direction.

Figure 2 shows the evolution of the structure dimensionality when $M = \tau_{\text{shear}}/\tau_m = 0.1$. Two different values of the magnetic Reynolds number ($R_m = 1$ and $R_m = 30$) are considered. In both cases, the magnetic interaction number is $N = 10$. The evolution of the dimensionality anisotropy is dominated by the mean shear and is independent of the R_m. At large times, $d_{11} \approx 0$, indicating a predominance of long streamwise eddies.

The evolution of the dimensionality anisotropy for $M = 20$ is shown in Figure 3. As expected, in this case the external spanwise magnetic field has a strong influence on the development of structure anisotropy. In the case when $R_m = 1$, the turbulence is driven towards a two-dimensional (2D) state corresponding to almost axisymmetric structures aligned with the direction of the magnetic field ($d_{33} \to 0$). Note however that when $R_m = 30$, the magnetic field is less effective in imposing the spanwise eddy alignment. In fact, at this moderately high R_m, the overall dimensionality anisotropy is suppressed as compared to the $R_m = 1$ case. There is also evidence that at large times the mean shear is contributing more effectively in the anisotropy development, and as a result d_{11} and d_{33} seem to decrease at approximately the same rate. This suggests that initially the structures become elongated in the spanwise direction under the action of the magnetic field. However, as the structures elongate the Joule dissipation becomes less effective, and this allows the shear to induce a streamwise elongation.

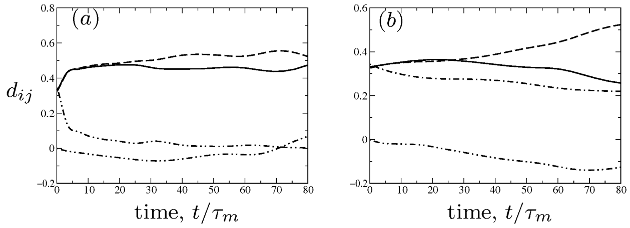

Figure 3: Evolution of the normalized dimensionality tensor in homogeneous MHD turbulence being sheared in a fixed frame ($\lambda = 0$) with $M = \tau_{\text{shear}}/\tau_m = 20$: ——— d_{11}; – – – – d_{22}; —·— d_{33}; —··— d_{12}. (a) Case C321 with $R_m = 1, N = 10$; (b) Case C3230 with $R_m = 30, N = 10$.

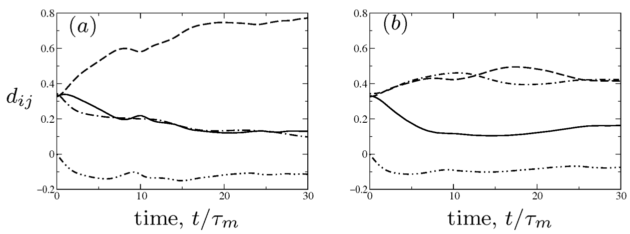

Figure 4: Evolution of the normalized dimensionality tensor in homogeneous MHD turbulence being sheared in a fixed frame ($\lambda = 0$) with $M = \tau_{\text{shear}}/\tau_m = 2$: ——— d_{11}; – – – – d_{22}; —·— d_{33}; —··— d_{12}. (a) Case C221 with $R_m = 1, N = 10$ (b) Case C2230 with $R_m = 30, N = 10$.

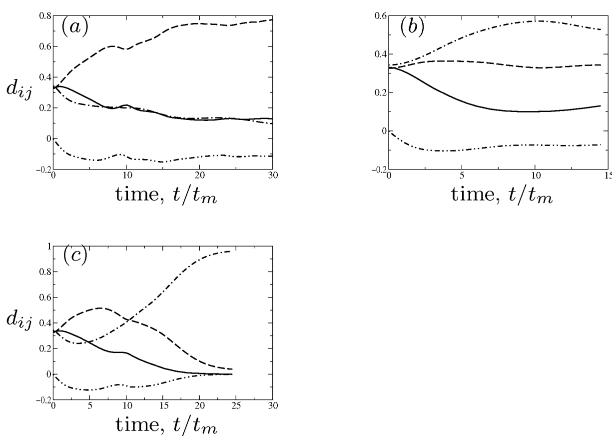

Figure 5: Evolution of the normalized dimensionality tensor in homogeneous MHD turbulence being sheared in a rotating frame with $M = \tau_{\text{shear}}/t_m = 2$: ——— d_{11}; – – – – d_{22}; —·— d_{33}; —··— d_{12}. (a) Case C221 with $R_m = 1, N = 10$, and $\lambda = 0$ (no rotation); (b) Case C221 with $B = 0$ and $\lambda = 0.25$ (hydrodynamic case); (c) Case 221 with $R_m = 1, N = 10$, and $\lambda = 0.25$.

A more interesting anisotropy evolution is obtained in the case when $M = 2$, that is when the mean shear time scale is comparable to the Joule time. Figure 4a shows the evolution of the dimensionality anisotropy when $R_m = 1$. In this case, $d_{11} \approx d_{33} \to 0$ suggesting that the mean shear and the external field are equally effective in inducing structural anisotropy. As result, at large times the turbulence is characterized by thin ($d_{22} \to 1$) horizontal sheets (see also Fig. 6a) . However, when $R_m = 30$ (Fig. 4b) the mean shear dominates, inducing long, roughly axisymmetric, eddies aligned with the streamwise direction ($d_{11} \to 0$).

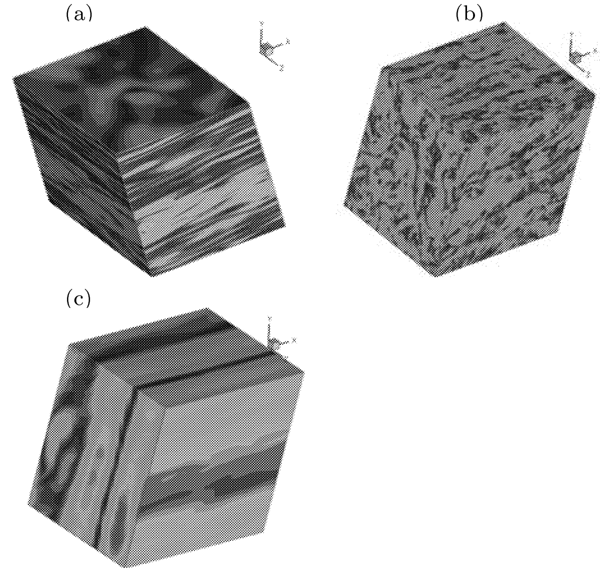

Figure 6: Velocity magnitude contours showing the structural anisotropy induced at large times by the combined action of spanwise frame rotation and spanwise mean magnetic field: (a) Case C221 ($M = 2, N = 10, R_m = 1$) with zero frame rotation. The structure is characterized by horizontal slabs (equal elongation in the streamwise and spanwise direction; (b) Case C221 with frame rotation rate $\lambda = 0.25$ and zero magnetic field (hydrodynamic case).

So far we have considered the evolution of structure anisotropy in a fixed frame. Figure 5 shows the development of the normalized dimensionality tensor in the rotating frame for the case $M = 2$, $N = 10$, and at $R_m = 1$. Figure 5a corresponds to $\lambda = 0$ and shows that in the fixed frame, the magnetic field and the mean shear are equally effective in inducing two-dimensionality, and as a result the structure evolves towards a state characterized by horizontal sheets (see also Fig. 6a). In a frame rotating about the spanwise axis at a rate $\lambda = 0.25$, and in the absence of an external magnetic field (hydrodynamic case), the structure evolves towards a state characterized by elongated streamwise eddies ($d_{11} \to 0$), as shown in Fig. 5b. Note however, that these eddies tend to be somewhat elongated in the x_2 direction, that is in the flow-normal direction within the frame of the mean shear ($d_{22} < d_{33}$). This flattening of the eddies is also evident in the structure visualization of Fig. 6b. An interesting bifurcation seems to take place in the case when the frame rotation and the external magnetic field act concurrently (Fig. 5c). At short times, the evolution of the normalized dimensionality tensor is similar to the one obtained in the non-rotating case, and reveals a balance between the effects of the mean shear and the external magnetic field. At larger times, however ($\tau/\tau_m \gtrsim 5$) a sudden transition takes place leading eventually to a state characterized by vertical slabs ($d_{11} \approx d_{22} \to 0$ and $d_{33} \to 1$).

5.2 Scale Dependence of Anisotropy

The scale dependence of anisotropy in incompressible MHD turbulence at moderate magnetic Reynolds numbers remains an open question. For compressible turbulence at high magnetic Reynolds numbers, Cho and Lazarian (2003) have found

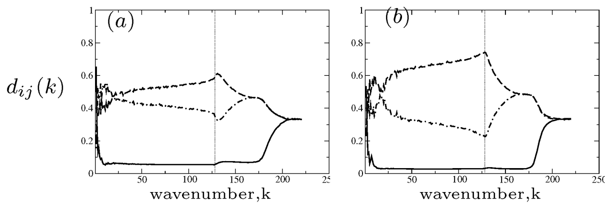

Figure 7: Scale dependence of anisotropy as measured by $d_{ij}(k)$ (see 17) in homogeneous MHD turbulence being sheared in a rotating frame: ——— $d_{11}(k)$; - - - - $d_{22}(k)$; —·— $d_{33}(k)$. (a) Case C2250 ($R_m = 50, N = 10, M = 2$) with $\lambda = 0.75$ and $t/t_m = 31.7$, and (b) Case C2250 ($R_m = 50, N = 10, M = 2$) with $\lambda = 1.0$ and $t/t_m = 38.0$.

that Alfven mode velocity fluctuations show a strong scale dependence, with the small scales being more anisotropic than the larger ones.

We have attempted to obtain a scale dependent measure of anisotropy using the spectra of the turbulence structure dimensionality tensor Kassinos et al.(2001). Thus we define

$$d_{ij}(k) = \sum_{\text{shell}} E(k)\frac{k_i k_j}{k^2} / \sum_{\text{shell}} E(k) \qquad d_{ii}(k) = 1\,, \tag{17}$$

where the summation in (17) is over shells in Fourier space. For turbulence that is isotropic at the scale set by k we have $d_{ij}(k) = \delta_{ij}/3$. For turbulence that it is two-dimensional (2D) independent of direction x_α, $d_{\alpha\alpha}(k) = 0$.

Figure 7 shows the anisotropy levels obtained for two cases with frame rotation (C2250 with $\lambda = 0.75$ and C2250 with $\lambda = 1.0$). Variations at very low wavenumbers are spurious and attributed to limited sample. On the other end of the spectrum, variations beyond $k \approx 128$ are again contaminated by the progressive loss of modes that extend beyond the limits of the computational box (for these 256^3 simulations). In the intermediate range that lies between these limits, anisotropy as measured by $d_{ij}(k)$ exhibits a weak increase with wave number, especially in the flow-normal directions. This trend is suggestive of the observations of Cho and Lazarian (2003) in compressible MHD turbulence at high R_m. Cases with low R_m did not seem to exhibit this increase of anisotropy with decreasing scale, but a more careful analysis for our results is needed in order to establish a possible Reynolds number dependence. Both cases correspond to $M = 2$, that is the time scale associated with the mean shear is twice as large as the time scale associated with the diffusion of the magnetic field. Yet, in both cases, $d_{11}(k) \approx 0$ for the entire range of wave numbers over which results are meaningful. Thus at these relatively high R_m, the mean shear seems to determine the overall structural anisotropy when the two time scales are comparable. Because of the limited size of the computational box, we were unable to adequately answer the question of anisotropy at small scales. We plan to carry a series of 512^3 simulations in order to address that question more thoroughly. We also hope that these higher-resolution simulations will allow us to clarify the slight increase of anisotropy that was observed in the cases discussed above.

6. CONCLUSIONS AND FUTURE PLANS

We have used direct numerical simulations to examine the structure of homogeneous MHD turbulence subjected to mean shear in fixed and rotating frames. We have found that the most interesting dynamics is observed when the time scale of the mean shear is comparable to that of the applied magnetic field. In this regime, the magnetic field and the mean shear exert competing influences on the structure of the turbulence and relatively small variations in the governing parameters seem to lead to markedly different evolving states. Counter to intuition we have found that the combined action of a spanwise mean magnetic field and spanwise frame rotation can lead to enhanced streamwise alignment of the turbulence structures. We have also found evidence that, at moderate magnetic Reynolds numbers, a week scale-dependence of structural anisotropy exists, with smaller structures being more evidently anisotropic than larger ones.

We hope this work will lead to an improved fundamental understanding of the combined effects of mean shear, frame rotation and magnetic fields on MHD turbulence. We plan to use this understanding for the development of improved structure-based models of MHD shear turbulence. A deeper understanding of the mechanisms that lead to instability and anisotropy in these flows is also important in the study of accretion in stellar disks and in engineering applications such as magnetogasdynamics.

REFERENCES

Cho, J., and Lazarian, A., 2003, "Compressible magnetohydrodynamic turbulence: mode coupling scaling relations, anisotropy, viscosity-damped regime and astrophysical implications." *Monthly Not. Royal Astron. Soc.*, Vol. 345, pp. 325-339.

Kassinos, S. C., Reynolds, W. C., and Rogers, M. M., 2001, "One-point turbulence structure tensors", *J. Fluid Mech.*, Vol. 428, pp. 213-248.

Kassinos, S. C., Knaepen, B., and Carati, D., 2002, "MHD turbulence at moderate magnetic Reynolds number", *Proceedings for the 2002 Summer Program, Center of Turbulence Research*, Stanford/NASA Ames.

Knaepen, B., Kassinos S. C., and Carati, D., 2004, "MHD turbulence at moderate magnetic Reynolds number", *J. Fluid Mech.*, Vol. 513, pp. 199-220.

Moffatt, H. K., 1967, "On the suppression of turbulence by a uniform magnetic field", *J. Fluid Mech.*, Vol. 28, pp. 571-592.

Roberts, P. H., 1967, "An Introduction to Magnetohydrodynamics", *Elsevier*, New York.

Rogers, M. M. and Moin, P., 1987, "The structure of the vorticity field in homogeneous turbulent flows", *J. Fluid Mech.*, Vol. 176, pp. 33-66.

Rogallo, R. S., 1981, "Numerical experiments in homogeneous turbulence", NASA Technical Memorandum 81315.